PERGAMON

International Journal of Heat and Mass Transfer 42 (1999) 2621–2627

International Journal of HEAT and MASS TRANSFER

Free convection boundary-layer flow along a vertical surface in a porous medium with Newtonian heating

D. Lesnic[a], D.B. Ingham[a,*], I. Pop[b]

[a] *Department of Applied Mathematics, University of Leeds, Leeds LS2 9JT, U.K.*
[b] *Faculty of Mathematics, University of Cluj, R-3400, Cluj, CP 253, Romania*

Received 13 August 1998

Abstract

In this paper the steady free convection boundary-layer flow along a vertical surface embedded in a porous medium with Newtonian heating is investigated. The mathematical problem reduces to a pair of coupled partial differential equations for the temperature and the streamfunction, and full numerical, asymptotic and matching solutions are obtained for a wide range of values of the coordinate along the plate. The results for the temperature profiles on the plate and in the convective fluid are presented. A comparison between the full finite-difference solution and the small and large series expansion solutions illustrates that the full numerical solution is accurate. Furthermore, a matching closed form of solution for the scaled temperature on the wall is fitted to the theoretical results and this will be useful in numerous engineering practical applications.

Nomenclature

g the magnitude of the acceleration due to gravity
h_s heat transfer coefficient
H scaled wall temperature
K permeability
l streamwise length scale
T temperature
T_∞ ambient temperature
$(\bar{u}, \bar{v})$ velocity components
U_c characteristic speed
$(\bar{x}, \bar{y})$ Cartesian coordinates.

Greek symbols
α thermal diffusivity
β coefficient of thermal expansion
$\Gamma(.\,,.)$ incomplete Gamma function
θ_w wall temperature
ν kinematic viscosity
ψ streamfunction.

1. Introduction

Heat transfer in saturated porous media has received growing interest during the last four decades. To a large extent, this interest is stimulated by the fact that thermally driven flows in porous media are of considerable practical applications in modern industry. These include the utilization of thermal energy, design of building components for energy consideration, control of pollutant spread in groundwater, design of nuclear reactors, solar power collectors, compact heat exchangers, food industries, to name just a few applications. An excellent review of existing theoretical and experimental work on this subject can be found in the recent monographs by Nield and Bejan [1] and Ingham and Pop [2].

The usual way in which thermal convection flows in porous media are modelled is to assume that the flow is driven either by a prescribed surface temperature or by a prescribed surface heat flux. Here a somewhat different driving mechanism for free convection along a vertical surface embedded in a porous medium is considered in that it is assumed that the flow is set up by a Newtonian heating from the surface. In particular, the heat transfer from the surface is taken to be proportional to the local surface temperature and this situation was recently considered by Merkin [3] for the corresponding problem of

* Corresponding author. Tel: 0044 0113 2335 113; fax: 0044 0113 2429 925.
E-mail address: amt6dbi@amsta.leeds.ac.uk (D. B. Ingham)

0017–9310/99/$ - see front matter
PII: S0017–9310(98)00251–8

a viscous (non-porous) fluid. It is worth mentioning that a similar situation to the present problem arises in conjugate convective flows, where the heat is supplied to the convecting fluid through a bounded surface with a finite heat capacity. Papers by Pop et al. [4], Vinnycky and Kimura [5, 6], Lesnic et al. [7], Pop and Merkin [8] and Higuera and Pop [9] have treated some aspects of the conjugate heat transfer effects in porous media and an excellent review article on this topic has been recently published by Kimura et al. [10].

A solution is obtained for the present situation following a method which is similar to that presented in the Refs [4, 7, 8]. Series expansions which are valid both near the leading edge and far downstream of the plate are first obtained. These two solution regions are then joined by a numerical solution of the full boundary-layer equations using a finite-difference scheme in combination with the method of continuous transformation proposed by Hunt and Wilks [11]. It is found that near the leading edge the flow is driven, at the first-order, by a constant heat flux from the surface, and the higher-order terms are then perturbations of the standard uniform heat flux solution which is the same behaviour seen in the corresponding conjugate problem. However, there is an essential difference between the present case and the conjugate problem when the solution far downstream is considered. Namely, for the conjugate problem, the flow far downstream approaches the standard isothermal wall solution, whilst for the present situation the flow far downstream gives rise to a new similarity solution which can be found analytically.

2. Basic equations

Consider the steady free convection flow along a vertical flat plate which is embedded in a porous medium at the ambient temperature T_∞. The flow is assumed to be set up by a heat transfer from the surface which is proportional to the local surface temperature, i.e.

$$\frac{\partial T}{\partial \bar{y}} = -h_s T, \quad \text{on} \quad \bar{y}=0 \quad (\bar{x}>0) \tag{1}$$

where $(\bar{x}, \bar{y})$ are the Cartesian coordinates measuring distances along and normal to the plate, T is the temperature and h_s is a constant heat transfer coefficient.

Based on the boundary-layer and Darcy–Boussinesq approximations, the governing equations are simplified to the following form:

$$\frac{\partial \bar{u}}{\partial \bar{x}} + \frac{\partial \bar{v}}{\partial \bar{y}} = 0 \tag{2}$$

$$\bar{u} = \frac{gK\beta}{\nu}(T - T_\infty) \tag{3}$$

$$\bar{u}\frac{\partial T}{\partial \bar{x}} + \bar{v}\frac{\partial T}{\partial \bar{y}} = \alpha \frac{\partial^2 T}{\partial \bar{y}^2} \tag{4}$$

which have to be solved subject to the boundary conditions

$$\bar{v}=0, \quad \frac{\partial T}{\partial \bar{y}} = -h_s T, \quad \text{on} \quad \bar{y}=0$$

$$\bar{u}\to 0, \quad T\to T_\infty, \quad \text{as} \quad \bar{y}\to\infty$$

$$\bar{u}=\bar{v}=0, \quad T=T_\infty, \quad \text{at} \quad \bar{x}=0. \tag{5}$$

Here $(\bar{u}, \bar{v})$ are the velocity components along the $(\bar{x}, \bar{y})$ axes, g is the magnitude of the acceleration due to gravity, K is the permeability of the porous medium, β is the coefficient of thermal expansion, α is the thermal diffusivity and ν is the kinematic viscosity.

Let us now introduce the following dimensionless variables

$$x=\bar{x}/l, \quad y=h_s\bar{y}, \quad u=\bar{u}/U_c, \quad v=lh_s\bar{v}/U_c,$$

$$\theta=(T-T_\infty)/T_\infty \tag{6}$$

where l is the streamwise length scale and U_c is a characteristic speed which are defined as

$$l=(gK\beta T_\infty)/(\alpha\nu h_s^2), \quad U_c=\alpha h_s^2 l. \tag{7}$$

Substituting the transformation (6) and (7) into Eqs. (2)–(4) leads to the non-dimensional equations

$$\frac{\partial u}{\partial x} + \frac{\partial v}{\partial y} = 0 \tag{8}$$

$$u=\theta \tag{9}$$

$$u\frac{\partial \theta}{\partial x} + v\frac{\partial \theta}{\partial y} = \frac{\partial^2 \theta}{\partial y^2} \tag{10}$$

and the boundary conditions (5) become

$$v=0, \quad \frac{\partial \theta}{\partial y} = -(1+\theta), \quad \text{on} \quad y=0$$

$$u\to 0, \quad \theta\to 0, \quad \text{as} \quad y\to\infty. \tag{11}$$

3. Solution

3.1. Solution for small x

Here the flow develops initially by the heat flux from the surface, which suggests the transformation, for a solution valid near the leading edge,

$$\psi(x,\eta)=x^{2/3}f(x,\eta), \quad \theta(x,\eta)=x^{1/3}h(x,\eta), \quad \eta=y/x^{1/3} \tag{12}$$

where ψ is the streamfunction which is defined in the

usual way as $u=\partial\psi/\partial y$ and $v=-\partial\psi/\partial x$. Using Eq. (12), we obtain $h=\partial f/\partial\eta$, and thus Eqs. (8)–(11) reduce to

$$\frac{\partial^3 f}{\partial\eta^3}+\frac{2}{\eta}f\frac{\partial^2 f}{\partial\eta^2}-\frac{1}{3}\left(\frac{\partial f}{\partial\eta}\right)^2=x\left(\frac{\partial f}{\partial\eta}\frac{\partial^2 f}{\partial\eta\,\partial x}-\frac{\partial f}{\partial x}\frac{\partial^2 f}{\partial\eta^2}\right) \tag{13}$$

with the boundary conditions

$$f=0,\quad \frac{\partial^2 f}{\partial\eta^2}=-\left(1+x^{1/3}\frac{\partial f}{\partial\eta}\right),\quad \text{on}\quad \eta=0$$

$$\frac{\partial f}{\partial\eta}\to 0,\quad \text{as}\quad \eta\to\infty. \tag{14}$$

These boundary conditions suggest looking for a solution of Eqs. (13) for small x of the form

$$f(x,\eta)=\sum_{j=0}^{\infty}x^{j/3}f_j(\eta) \tag{15}$$

where f_0 is given by

$$f_0'''+\frac{2}{3}f_0f_0''-\frac{1}{3}f_0'^2=0$$

$$f_0(0)=0,\quad f_0''(0)=-1,\quad f_0'(\infty)=0 \tag{16}$$

and for $j\geqslant 1$, we have the following:

$$f_j'''+\sum_{p=0}^{j}\left[\left(\frac{j-p+2}{3}\right)f_{j-p}f_p''-\frac{(p+1)}{3}f_{j-p}'f_p'\right]=0$$

$$f_j(0)=0,\quad f_j'(0)=-f_{j-1}'(0),\quad f_j'(\infty)=0. \tag{17}$$

Here the primes denote the differentiation with respect to η. Eqs. (16) and (17) for $j=\overline{1,6}$, have been solved numerically using the NAG routine D02HBF [12], to obtain the small x temperature at the wall as

$$\begin{aligned}\theta_{\omega}^{(s)}(x)&=x^{1/3}f_0'(0)+x^{2/3}f_1'(0)+xf_2'(0)+x^{4/3}f_3'(0)\\&\quad+x^{5/3}f_4'(0)+x^2f_5'(0)+x^{7/3}f_6'(0)+\ldots\\&=1.2959x^{1/3}+0.9515x^{2/3}+0.4429x+0.1187x^{4/3}\\&\quad+6.4429\times10^{-3}x^{5/3}-6.4451\times10^{-3}x^2\\&\quad-9.4502\times10^{-4}x^{7/3}+\ldots\end{aligned} \tag{18}$$

Eq. (16) for the leading-order term f_0 gives the uniform heat flux solution. The numerically retrieved value of $f_0'(0)=1.2959$ is in very good agreement with the values 1.2961 and 1.2953 which have been previously obtained by Rees and Pop [13] and Kumari et al. [14], respectively.

3.2. Solution for large x

In this case we take

$$\psi=x\tilde{f}(x,y),\quad \theta=x\tilde{h}(x,y). \tag{19}$$

On applying the transformation (19) to Eqs. (8)–(11) yields $\tilde{h}=\partial\tilde{f}/\partial y$ and $\tilde{f}$ is determined from the equation

$$\frac{\partial^3\tilde{f}}{\partial y^3}+\tilde{f}\frac{\partial^2\tilde{f}}{\partial y^2}-\left(\frac{\partial\tilde{f}}{\partial y}\right)^2=x\left(\frac{\partial\tilde{f}}{\partial y}\frac{\partial^2\tilde{f}}{\partial y\,\partial x}-\frac{\partial\tilde{f}}{\partial x}\frac{\partial^2\tilde{f}}{\partial y^2}\right) \tag{20}$$

along with the boundary conditions

$$\tilde{f}=0,\quad \frac{\partial^2\tilde{f}}{\partial y^2}=-\frac{\partial\tilde{f}}{\partial y}-x^{-1},\quad \text{on}\quad y=0$$

$$\frac{\partial\tilde{f}}{\partial y}\to 0,\quad \text{as}\quad y\to\infty. \tag{21}$$

These boundary conditions suggest looking for a solution of Eq. (20) of the form

$$\tilde{f}(x,y)=\tilde{f}_0(y)+x^{-1}[\ln(x)\phi_1(y)+\tilde{f}_1(y)]+\ldots \tag{22}$$

where the $\mathbf{O}(x^{-1})$ term includes the eigensolution ϕ_1 due to the leading edge shift effect as mentioned by Stewartson [15]. The functions $\tilde{f}_0$, ϕ_1 and $\tilde{f}_1$ are given by the following ordinary differential equations:

$$\tilde{f}_0'''+\tilde{f}_0\tilde{f}_0''-\tilde{f}_0'^2=0,$$

$$\tilde{f}_0(0)=0,\quad \tilde{f}_0''(0)=-\tilde{f}_0'(0),\quad \tilde{f}_0'(\infty)=0 \tag{23}$$

$$\phi_1'''+\tilde{f}_0\phi_1''-\tilde{f}_0'\phi_1'=0,$$

$$\phi_1(0)=0,\quad \phi_1''(0)=-\phi_1'(0),\quad \phi_1'(\infty)=0 \tag{24}$$

$$\tilde{f}_1'''+\tilde{f}_0\tilde{f}_1''-\tilde{f}_0'\tilde{f}_1'-\tilde{f}_0'\phi_1'+\tilde{f}_0''\phi_1=0$$

$$\tilde{f}_1(0)=0,\quad \tilde{f}_1''(0)=-\tilde{f}_1'(0)-1,\quad \tilde{f}_1'(\infty)=0 \tag{25}$$

where now the primes denote differentiation with respect to y. From Eqs. (23) and (24), the term ϕ_1 can be expressed as

$$\phi_1=a_0\tilde{f}_0 \tag{26}$$

for, as yet, an undetermined constant a_0. Introducing Eq. (26) into Eq. (25) and using Eq. (23) yields

$$\tilde{f}_1'''+\tilde{f}_0\tilde{f}_1''-\tilde{f}_0'\tilde{f}_1'=a_0\tilde{f}_0'''$$

$$\tilde{f}_1(0)=0,\quad \tilde{f}_1''(0)=-\tilde{f}_1'(0)-1,\quad \tilde{f}_1'(\infty)=0. \tag{27}$$

Eqs. (23) and (27) can be solved analytically to give

$$\tilde{f}_0(y)=1-e^{-y},\quad \phi_1(y)=a_0(1-e^{-y}) \tag{28}$$

$$\begin{aligned}\tilde{f}_1(y)&=a_0(1-y)-e^{-y}-a_0e^{-e^{-y}}\\&\quad+a_0(1+e^{-y})(\Gamma(0,e^{-y})-\Gamma(0,1))+c(1-e^{-y})\end{aligned} \tag{29}$$

where c is an undetermined constant, $a_0=e/(e-1)$ and

$$\Gamma(a,x)=\int_x^{\infty}e^{-t}t^{a-1}\,\mathrm{d}t,\quad \frac{\mathrm{d}\Gamma}{\mathrm{d}x}(a,x)=-x^{a-1}e^{-x} \tag{30}$$

is the incomplete Gamma function. Therefore, the solu-

tion (22) is not fully determined to this order, as arbitrary multiples of the eigensolution (28) can be added. Thus, the wall temperature for large x is given by

$$\theta_w^{(j)}(x)=\tilde{f}'_0(0)x+\frac{e}{e-1}\tilde{f}'_0(0)\ln(x)+\tilde{f}'_1(0)+\ldots$$

$$=x+\frac{e}{e-1}\ln(x)+c+\ldots \quad (31)$$

3.3. Numerical solution

To obtain a numerical solution of Eqs. (8)–(11) that hold for all values of x, starting at $x=0$ and proceeding downstream until the asymptotic solution given by Eq. (30) is attained, we use the method of continuous transformation [11]. Thus, applying the transformation

$$\psi(x,\zeta)=x^{2/3}(1+x)^{1/3}F(x,\zeta),$$

$$\theta(x,\zeta)=x^{1/3}(1+x)^{2/3}H(x,\zeta),\quad \zeta=yx^{-1/3}(1+x)^{1/3} \quad (32)$$

to Eqs. (8)–(10) yields $H=\partial F/\partial\zeta$ and F is determined from the equation

$$\frac{d\partial^3 F}{\partial\zeta^3}+\frac{(2+3\xi^3)}{(3+3\xi^3)}F\frac{\partial^2 F}{\partial\zeta^2}-\frac{(1+3\xi^3)}{(3+3\xi^3)}\left(\frac{\partial F}{\partial\zeta}\right)^2$$

$$=\frac{\xi}{3}\left(\frac{\partial F}{\partial\zeta}\frac{\partial^2 F}{\partial\zeta\,\partial\xi}-\frac{\partial F}{\partial\xi}\frac{\partial^2 F}{\partial\zeta^2}\right) \quad (33)$$

where to accommodate for the $x^{1/3}$ singularity as $x\to 0$, we have used the variable $\xi=x^{1/3}$ as the streamwise variable. The transformed boundary conditions (11) become

$$F(\xi,0)=0,\quad \frac{\partial^2 F}{\partial\zeta^2}(\xi,0)+\xi(1+\xi^3)^{-1/3}\frac{\partial F}{\partial\zeta}(\xi,0)$$

$$=-(1+\xi^3)^{-1},\quad \frac{\partial F}{\partial\zeta}(\xi,\infty)=0. \quad (34)$$

Finally, the wall temperature is given by

$$\theta_w(x)=x^{1/3}(1+x)^{2/3}\frac{\partial F}{\partial\zeta}(x,0). \quad (35)$$

It should be noted that Eqs. (32)–(34) reduce to Eqs. (12)–(14) for small values of x, and to Eqs. (19)–(21) for large values of x. The fluid velocity and the heat flux on the wall are given by

$$u_w(x)=x^{-1/3}(1+x)^{1/3}\frac{\partial F}{\partial\zeta}(x,0) \quad (36)$$

$$q_w(x)=x^{-2/3}(1+x)^{2/3}\frac{\partial H}{\partial\zeta}(x,0). \quad (37)$$

Eqs. (33) and (34) have been solved numerically using a modification of the finite-difference method of Merkin [16].

4. Results and discussion

Fig. 1 shows the full numerical solution of Eqs. (33) and (34) for the scaled temperature on the wall $H(\xi,0)=\xi^{-1}(1+\xi^3)^{-2/3}\theta_w(\xi)$, plotted against $\xi=x^{1/3}$, in comparison with the small values of ξ solution, see Eq. (18),

$$h_w^{(j)}(\xi)=(1+\xi^3)^{-2/3}\sum_{i=0}^{j}\xi^i f'_i(0) \quad (38)$$

for $j=\overline{0,6}$, and with the large values of ξ solution, see Eq. (31),

$$h_w^{(l1)}(\xi)=\xi^2(1+\xi^3)^{-2/3} \quad (39)$$

$$h_w^{(l2)}(\xi)=\xi^2(1+\xi^3)^{-2/3}$$

$$+\frac{3e}{e-1}\xi^{-1}(1+\xi^3)^{-2/3}\ln(\xi). \quad (40)$$

From Fig. 1 it can be seen that as more terms from $j=0$ to $j=3$ are considered in the series expansion (38), the better is the agreement with the full numerical solution for small values of ξ. In fact, the $(j+1)$-terms small ξ solution (38) can be used approximately up to $\xi=0.1$, 0.3, 0.7 and 2 for $j=0$, 1, 2 and 3, respectively. By taking more than four terms in the series expansion (38) the agreement with the full numerical solution is only slightly improved for small values of ξ and, in fact, only the six-terms small solution is slightly better than the four-terms small solution and it can be used up to $\xi\leqslant 2.25$ within an error of less than 1% from the full numerical solution. From this we can conclude that between 4–7 terms are sufficient to be considered in solving Eq. (17) for small values of ξ. At large values of ξ, the one-term large ξ

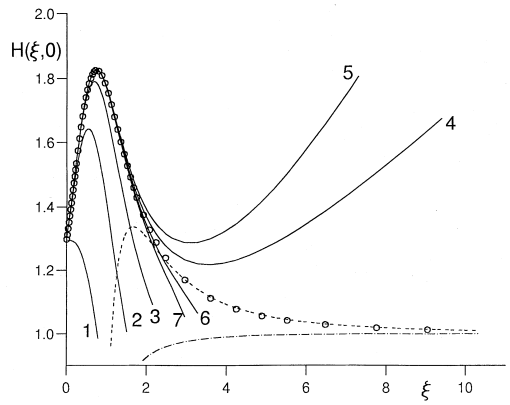

Fig. 1. The scaled wall temperature $H(\xi,0)=\xi^{-1}(1+\xi^3)^{-2/3}\theta_w(\xi)$ as obtained from the full numerical solution of Eqs. (33) and (34) (o o o), plotted against $\xi=x^{1/3}$, in comparison with the $(j+1)$-terms small values of ξ solution (38) for $j=\overline{0,6}$, and with the one-term (- · -) and two-terms (- - -) large values of ξ solutions (39) and (40).

solution (39) approaches asymptotically the scaled full numerical solution which tends to unity as $\xi\to\infty$. However, when the logarithmic term is taken into account it can be seen that the two-terms large ξ solution (40) is a significant improvement and it can be used for $\xi\geqslant 2.5$ with an error of less than 1% from the full numerical solution. It is only in the range $2.25<\xi<2.5$ that it may be considered necessary to use the full numerical solution in order to obtain an accurate solution. However, it is worth noting that at the point of intersection $\xi\approx 2.4$ of the curves $h_w^{(5)}(\xi)$ and $h_w^{(I2)}(\xi)$, where the largest deviation from the full numerical solution $H(\xi,0)$ occurs, the relative error is less than 3%.

Further, in order to investigate whether the convergence of the series (18) can be accelerated we apply the Shanks method [17] namely, instead of the partial sum (38) we consider the sequence

$$e_i^n=\frac{e_{i+1}^{n-1}e_{i-1}^{n-1}-(e_i^{n-1})^2}{e_{i+1}^{n-1}+e_{i-1}^{n-1}-2e_i^{n-1}},\quad n=\overline{1,m},\quad i=\overline{n,(2m-n)} \tag{41}$$

where $m=j/2$, $j=2$, 4 or 6 and $e_i^0=\theta_w^{(i)}$ for $i=\overline{0,j}$.

Fig. 2 shows the numerical results for the full numerical solution of Eqs. (33) and (34) for the scaled temperature on the wall $H(\xi,0)$ in comparison with the corresponding scaled Shanks solutions (41) for $j=2$, 4 and 6. From this figure it can be seen that only for $j=2$ does the Shanks method accelerate slightly the convergence of the series (38), whilst for higher values of j such as 4 or 6 the speed of convergence is not significant.

Fig. 3 shows the temperature profiles $\theta(\xi,\zeta)$ as obtained from the full numerical solution of Eqs. (33) and (34), plotted on a linear-log scale as a function of ζ, for various values of $\xi=x^{1/3}=0.1075$, 0.4975, 0.7575, 0.9975, 2.4775, 4.8775, 7.7575, 10.3175 and 15.4375. From this figure it can be seen that the temperature

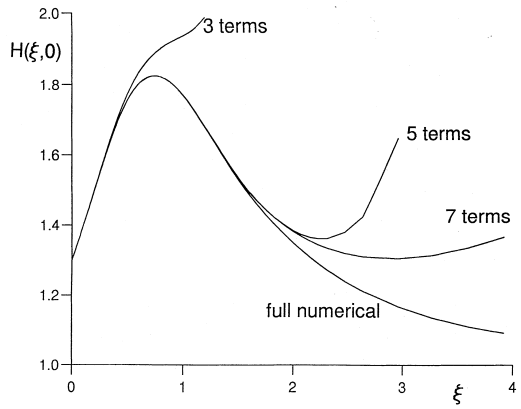

Fig. 2. The scaled wall temperature $H(\xi,0)=\xi^{-1}(1+\xi^3)^{-2/3}\theta_w(\xi)$ as obtained from the full numerical solution of Eqs. (33) and (34), plotted against $\xi=x^{1/3}$, in comparison with the Shanks solutions (41) for $j=2$, 4 and 6.

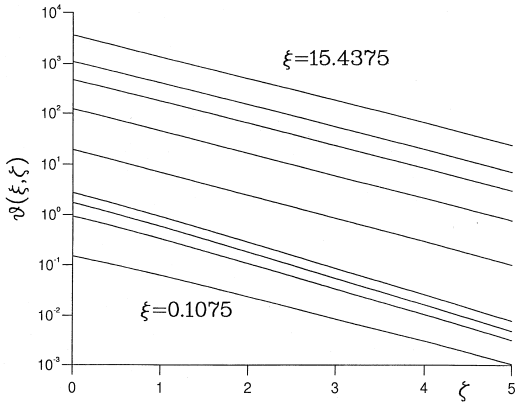

Fig. 3. Temperature profiles $\theta(\xi,\zeta)$ as obtained from the full numerical solution of Eqs. (33) and (34), plotted against ζ, for various values of $\xi=0.1075$, 0.4975, 0.7575, 0.9975, 2.4775, 4.8775, 7.7575, 10.3175 and 15.4375 (as ξ increases the curves increase).

profiles, as a function of ζ, decrease towards the zero profile as ξ decreases to zero, whilst for large values of ξ they behave like the large solution profile, see Eqs. (19), (31) and (32), namely,

$$\theta^{(l)}(\xi,\zeta)=\xi^3\exp(-\zeta\xi(1+\xi^3)^{-1/3}). \tag{42}$$

Although not presented in the paper, it is interesting to note that for $\zeta<5$ the results presented in Fig. 3 agree within 1% with the six-terms small ξ solution (15) for $\xi\leqslant 2.25$, and with the two-terms large ξ solution (22) for $\xi\geqslant 2.5$.

Finally, for engineering practical purposes, the full numerical solution for the scaled temperature on the wall $H(\xi,0)$ is compared with a much simpler scaled matching solution. These matching solutions are not unique but rather than having to perform a complete full numerical solution, it is sometimes useful, for engineering purposes, to seek a closed form approximate solution which may be used with confidence over the whole interval range of interest. For example, looking for a matching solution which agrees with the five-terms small ξ solution $h_w^{(4)}(\xi)$ as $x\to 0$, and with the two-terms the large ξ solution $h_w^{(I2)}(\xi)$ as $x\to\infty$, we obtain the following matching solution:

$$H(\xi)=\frac{\xi(1+A\xi+B\xi^2+C\xi^3+D\xi^4+\xi^5)}{E+C\xi+D\xi^2+\xi^3}+\frac{3e}{e-1}\ln(\xi+1) \tag{43}$$

where

$$A=-55.9531,\quad B=13.9632,\quad C=15.9388,$$
$$D=11.4071,\quad E=-0.2988. \tag{44}$$

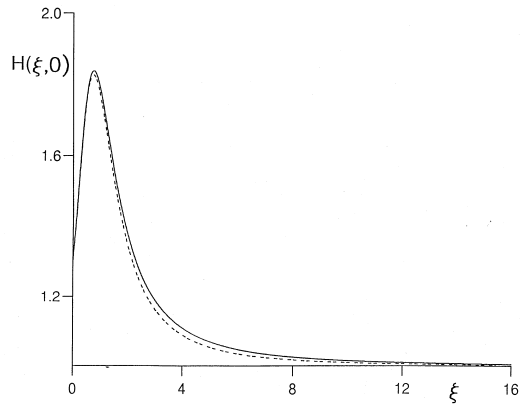

Fig. 4. The scaled wall temperature $H(\xi,0)=\xi^{-1}(1+\xi^3)^{-2/3}\theta_w(\xi)$ as obtained from the full numerical solution of Eqs. (33) and (34) (- - -), plotted against $\xi=x^{1/3}$, in comparison with the matching solution (43) (—).

Many other best fitted matching solutions which agrees with the solution (38) for small ξ and with the solutions (39) or (40) for large ξ, have been investigated, but they were found less accurate than the solution (43) over the whole range of values of ξ. In deriving the empirical formula (43), Maclaurin series expansions valid for small values of ξ were used to obtain agreement with the power series coefficients of $h_w^{(4)}(\xi)$, whilst for large values of ξ the coefficients of the Maclaurin series for the first term of the right-hand side of Eq. (43) transformed via the change of variables $\xi'=\xi^{-1}$, were chosen such that the coefficients in the powers of ξ and ξ^2 vanish. Based on this procedure, the computation of the coefficients given by Eq. (44) was made using MAPLE. The comparison made in Fig. 4 between the empirical formula (43) and the full numerical solution of Eqs. (33) and (34) shows that the former matching solution can be used with confidence over the whole range of values of ξ within 1–2% relative error and therefore may be used with confidence in engineering applications.

5. Conclusions

In this paper a comparison between the small, large and full numerical solutions of the free convection boundary-layer equations for a vertical plate embedded in a porous medium with Newtonian heating has been considered. We have found that, unlike in the viscous (non-porous) fluid flow situation considered by Merkin [3], the asymptotics for the large values of ξ solution, which occurs due to the leading edge effect, can be found analytically.

The numerical analysis shows that the full numerical solution is very accurate. The six-terms small ξ solution can be used between $0\leqslant\xi\leqslant2.25$, whilst the two-terms large ξ solution, which includes a logarithmic behaviour, can be used from $\xi\geqslant2.5$. Between these limits the full numerical solution could be employed if accuracies less than 3% are required.

In order to accelerate the rate of convergence of the small ξ solution, the Shanks method has been employed but it was found that only the three-terms solution can be slightly improved by this technique.

Finally, for engineering applicability a simple matching solution for the scaled wall temperature which agrees within 1–2% with the full numerical solution, as given by Eq. (43), has been provided.

Future work will be concerned with investigating the analogous horizontal plate situation.

Acknowledgements

Professors D. B. Ingham and I. Pop gratefully acknowledge some financial support for this research from The Royal Society.

References

[1] D.A. Nield, A. Bejan, in: Convection in Porous Media, 2nd ed., Springer-Verlag, Berlin, 1998.
[2] D.B. Ingham, I. Pop (Eds.), Transport Phenomena in Porous Media, Elsevier, Amsterdam, 1998.
[3] J.H. Merkin, Natural convection boundary-layer flow on a vertical surface with Newtonian heating, Int. J. Heat Fluid Flow 15 (1994) 392–398.
[4] I. Pop, D. Lesnic, D.B. Ingham, Conjugate mixed convection on a vertical surface in a porous medium, Int. J. Heat Mass Transfer 38 (1995) 1517–1525.
[5] M. Vynnycky, S. Kimura, Conjugate free convection due to a vertical plate in a porous medium, Int. J. Heat Mass Transfer 37 (1994) 229–236.
[6] M. Vynnycky, S. Kimura, Transient conjugate free convection due to a vertical plate in a porous medium, Int. J. Heat Mass Transfer 38 (1995) 219–231.
[7] D. Lesnic, D.B. Ingham, I. Pop, Conjugate free convection from a horizontal surface in a porous medium, J. Appl. Math. Mech. (ZAMM) 75 (1995) 715–722.
[8] I. Pop, J.H. Merkin, Conjugate free convection on a vertical surface in a saturated porous medium, Fluid Dynamics Res. 16 (1995) 71–86.
[9] F.J. Higuera, I. Pop, Conjugate natural convection heat transfer between two porous media separated by a vertical wall, Int. J. Heat Mass Transfer 40 (1997) 123–129.
[10] S. Kimura, T. Kiwata, A. Okajima, I. Pop, Conjugate natural convection in porous media, Adv. Water Resour. 20 (1997) 11–126.
[11] R. Hunt, G. Wilks, Continuous transformation computation of boundary-layer equations between similarity regimes, J. Comput. Phys. 40 (1981) 478–490.
[12] I. Gladwell, The development of the boundary value codes in the ordinary differential equations, in: B. Childs, M. Scott, J.W. Daniel, E. Denman, P. Nelson (Eds.), Codes

for Boundary Value Problems in Ordinary Differential Equations, Springer-Verlag, Berlin, 1979.
[13] D.A.S. Rees, I. Pop, Free convection induced by a vertical wavy surface with uniform flux in a porous medium, J. Heat Transfer 117 (1995) 547–550.
[14] M. Kumari, I. Pop, G. Nath, Natural convection in porous media above a near horizontal uniform heat flux surface, Warme- und Stoffuber. 25 (1990) 155–159.
[15] K. Stewartson, On asymptotic expansions in the theory of boundary layers, J. Math. Phys. 36 (1957) 173–191.
[16] J.H. Merkin, Free convection boundary layer on an isothermal horizontal cylinder, ASME–AIChE National Heat Transfer Conference, Paper No. 76-HT-16, St. Louis, U.S.A. (1976).
[17] D. Shanks, Non-linear transformations of divergent and slowly convergent sequences, J. Maths. Phys. 34 (1995) 1–42.